GENOMICS 23, 100–113 (1994)

Integrated Mapping Analysis of the Werner Syndrome Region of Chromosome 8

JUNKO OSHIMA,* CHANG-EN YU,† MICHAEL BOEHNKE,‡ JAMES L. WEBER,§ SUSANNE EDELHOFF,* MICHAEL J. WAGNER,¶ DAN E. WELLS,¶ STEPHEN WOOD,‖ CHRISTINE M. DISTECHE,* GEORGE M. MARTIN,* AND GERARD D. SCHELLENBERG†,[1]

*Department of Pathology and the †Division of Neurology, University of Washington, Seattle, Washington 98195; ‡Department of Biostatistics, University of Michigan, Ann Arbor, Michigan 48109-2029; §Marshfield Medical Research Foundation, Marshfield, Wisconsin 54449; ¶Department of Biology and Institute for Molecular Biology, University of Houston, Texas 77204-5513; ‖Department of Medical Genetics, University of British Columbia, Vancouver, British Columbia, Canada V6T 1Z3

Received February 9, 1994; revised June 10, 1994

The Werner syndrome locus (WRN) is located at 8p11–p12. To facilitate eventual cloning of the WRN gene, a 10,000-rad radiation-reduced hybrid (RH) cell panel was generated to map genetic markers, sequence-tagged sites (STSs), and genes in this region. A hamster cell line carrying an intact human chromosome 8 was fused with another hamster cell line. Two sets of hybrid cell panels from 2 separate fusions were generated; each panel consisted of 50 independent clones; 33 and 34 cell lines from the 2 fusions retained human chromosome material as determined by inter-*Alu* PCR. The combined panel was genotyped for 52 markers spanning the entire chromosome, including 10 genes, 29 anonymous polymorphic loci, and 13 STSs. Seventeen of these markers have not been previously described. Markers near the centromere were retained at a higher frequency than more distal markers. Fluorescence *in situ* hybridization was also used to localize and order a subset of the markers. A RH map of the WRN region was constructed using a maximum likelihood method, giving the following most likely order: D8S131 – D8S339 (GSR) – D8S124 – D8S278 – D8S259 – (D8S71) – D8S283 – D8S87 – D8S105 – D8S135 (FGFR1) – D8S135PB–D8S255–ANK1. A genetic map of 15 short tandem repeat polymorphic loci in the WRN region was also constructed. The marker orders from the genetic and RH maps were consistent. In addition, an integrated map of 24 loci in the WRN region was generated using information from both genetic and RH mapping methods. A 1000:1 framework map for 6 loci (LPL–D8S136–D8S137–D8S87–FGFR1–ANK1) was determined by genetic mapping, and the resulting locus order was fixed during analysis of the RH genotype data. The resulting integrated map contained more markers than could confidently be ordered by either genetic or RH mapping alone. © 1994 Academic Press, Inc.

INTRODUCTION

Werner syndrome (WS) is a rare autosomal recessive disorder with a complex phenotype that may have components related to aging. WS subjects prematurely develop some of the physical features normally associated with aging, including gray hair, baldness, and skin atrophy. They also develop some of the major diseases of the elderly, including diabetes mellitus, several forms of heart disease, some benign and malignant neoplasms (particularly sarcomas), cataracts, and osteoporosis (Epstein *et al.*, 1966; Tollefsbol and Cohen, 1984). *In vitro* studies of fibroblast growth characteristics also suggest that WS may be related to aging. Primary fibroblasts from young donors are capable of undergoing more doublings prior to senescence when compared to cells from older donors. Fibroblasts from WS subjects have a limited growth potential and thus resemble cells from older donors (Salk *et al.*, 1985). This alteration in growth potential may be related to the hypermutator phenotype observed in WS fibroblasts (Fukuchi *et al.*, 1989, 1990). Recently, the WS gene (WRN) was assigned to human chromosome 8p11–p12 by conventional linkage analysis (Goto *et al.*, 1992). This localization was confirmed using an independent family set and homozygosity mapping methods (Schellenberg *et al.*, 1992a). The most likely location reported for the WRN locus was between D8S87 and ankyrin (ANK1; Goto *et al.*, 1992; Nakura *et al.*, 1993); D8S339 is the closest known marker (Thomas *et al.*, 1993).

In addition to WRN, loci for at least 8 other diseases have been mapped to chromosome 8. For 2 of these, the responsible genes have been identified. Mutations in ANK1 (8p11.1–p21.1) are responsible for hereditary

[1] To whom correspondence and reprint requests should be addressed at the Division of Neurology RG-27, University of Washington, Seattle, WA 98195. Telephone: (206) 543-2340. Fax: (206) 685-8100.

0888-7543/94 $6.00

spherocytosis (Lux *et al.,* 1990), and mutations in lipoprotein lipase (LPL) are involved in familiar hyperlipidemia type 1 in some families (Heinzmann *et al.,* 1991). Other disease loci localized to chromosome 8 include branchio-oto-renal syndrome at 8q11.2–p12 between D8S260 and D8S279 (Smith *et al.,* 1992; Kumar *et al.,* 1992), tricho-rhino-phalangeal syndrome type II (Langer–Giedion syndrome), and multiple exostosis at 8q24.1 (Parrish *et al.,* 1991; Cook *et al.,* 1993), retinitis pigmentosa (RP1) at 8q12–q21.3 (Blanton *et al.,* 1991), Charcot–Marie–Tooth type 4 (CMT4) at 8q13–q21.1 between D8S279 and D8S84 (Ben Othamane *et al.,* 1993), and benign familial neonatal convulsions (epilepsy, benign neonatal, EBN2) at 8q24 (Lewis *et al.,* 1993). Putative loci for prostate, colorectal, and lung cancers at 8p21–p22 have been suggested by loss of heterozygosity of this region in some tumors (Cunningham *et al.,* 1993; Chang *et al.,* 1994a).

Several genetic maps of chromosome 8 spanning the WRN locus have recently been published (Tomfohrde *et al.,* 1992; NIH/CEPH Collaborative Mapping Group, 1992; Emi *et al.,* 1992, 1993; Weissenbach *et al.,* 1992). Although some regions of chromosome 8 are densely covered, gaps without polymorphic markers exist (e.g., telomeric to D8S87). To improve the information about marker order and spacing in the WRN region, we generated a chromosome 8 radiation hybrid (RH) panel. A high density of markers in the WRN region were genotyped, including polymorphic loci, genes, and sequence-tagged sites (STSs). A genetic map of 14 short tandem repeat polymorphic (STRP) loci in the WRN region was also constructed. The resulting maps will facilitate locating new markers in the WRN region and eventual cloning of the gene. Also, the RH panel will be useful for mapping other regions of chromosome 8.

MATERIALS AND METHODS

Cell lines and culture conditions. GM10156B is a Chinese hamster–human hybrid cell line containing human chromosome 8 as the only human chromosome. Examination of metaphase chromosomes showed 1 intact human chromosome 8 per cell in all cells examined ($n = 20$). GM459A is a near-diploid Chinese hamster cell line deficient for hypoxanthine-guanine phosphoribosyl transferase (HPRT) activity. Both cell lines were obtained from the NIGMS Human Cell Repository (Camden, NJ). GM10156B was maintained in Ham's F12D medium supplemented with 6% dialyzed fetal calf serum (FCS) (Gibco-BRL), 3×10^{-5} *M* hypoxanthine, and antibiotics. GM459A was maintained in Dulbecco's modified Eagle's medium (DMEM) supplemented with 10% FCS, 6 μg/ml 6-thioguanine, and antibiotics.

RH cell lines were produced as previously described (Cox *et al.,* 1989; Siden *et al.,* 1992). Briefly, GM10156B and GM459A (2×10^7 cells each) were trypsinized, washed, and resuspended in 10 ml of serum-free DMEM. GM10156B cells were exposed to 10,000 rads of γ-irradiation at 2 rads/s on ice. After irradiation, the cell lines were mixed, collected by centrifugation, and fused in 0.5 ml of 50% (w/v) polyethylene glycol-1000 for 1 min. The fused cells were washed and incubated at 37°C for 90 min in 5 ml of DMEM. After centrifugation, cells were resuspended and plated in 60×100-cm^2 dishes in DMEM containing 10% FCS, 100 μM hypoxanthine, 1 μM aminopterin, and 12 μM thymidine (HAT). HAT medium was changed every 3–7 days for 3 weeks. For each fusion, 720 HAT-resistant colonies were isolated using cloning cylinders and transferred to 24-well plates. For the 1st fusion, cultures in 41 wells became confluent and were expanded and analyzed; 24 of 41 (59%) contained human sequences (either inter-*Alu* positive or positive for another human marker, ANK1). For the remaining wells, the culture was maintained for an additional week in medium containing 1/10 concentration of HAT; after 1 week, clones in 62 wells were confluent; 8 of 62 (13%) were *Alu*-positive. These results indicated that reducing the HAT concentration did not yield additional hybrid clones, but probably allowed HPRT$^-$ cells to grow. Thus, for the second fusion, only cells grown in 1× HAT were expanded and analyzed; 34 of 50 (68%) were *Alu*-positive.

Polymerase chain reaction (PCR) and genotyping analysis. Genomic DNA (100 ng) was amplified by PCR in 50 m*M* KCl, 10 m*M* Tris–HCl, pH 9.0, 1.0–3.0 m*M* $MgCl_2$ (depending on the primer set used), 0.1% Triton X-100, 0.2 m*M* dNTP, and 1 U *Taq* DNA polymerase in a final volume of 25 μl. Thermocycling conditions were as follows: an initial denaturation step at 94°C for 5 min; 3 amplification cycles at 94°C, 45–60°C (depending on the primer set), and 72°C for 1, 1, and 2 min, respectively; 30 amplification cycles at 94°C, 45–60°C (depending on the primer set used), and 72°C, for 0.5, 0.5, and 1 min, respectively; and a final extension step at 72°C for 10 min. Reaction products were separated by electrophoresis in 3% NuSieve agarose gel electrophoresis in 1X TBE. Bands were visualized by ethidium bromide staining. Analysis of PCR products was also performed using ^{32}P-radiolabeled oligonucleotide primers as previously described (Schellenberg *et al.,* 1992b). For loci used for RH map construction, the analysis was repeated at least 2 times. Controls of rodent DNA from the original cell lines used for the fusions were included to determine whether the PCR reactions were specifically amplifying human sequences. Inter-*Alu* PCR was performed as described by others using a combination of primers *Alu* TC-65 (Nelson *et al.,* 1989) or L1Hs (Ledbetter *et al.,* 1990). These primers gave no signal with hamster DNA. PCR primers for specific loci are described or referenced in Table 1.

Multipoint mapping of the radiation hybrid data. The chromosome 8 radiation hybrid mapping data were analyzed using a multipoint maximum likelihood method (Boehnke *et al.,* 1991). X-ray breakage was assumed to occur at random along the chromosome, and the resulting fragments were assumed to be independently retained in each radiation hybrid. In the *N*-locus case, the likelihood of the radiation hybrid data is a function of the *N*-1 breakage probabilities between adjacent loci and one or more fragment retention probabilities. We made use of data on all loci simultaneously, including information on partially typed hybrids.

To describe the different fragment retention probability models, let r_{ij} be the probability of retaining a fragment on which only loci $i < i + 1 < \cdots < j$ are present. We considered two such models. In the first, all fragment retention probabilities are assumed to be equal ($r_{ij} = r$ for all $i \leq j$). In the second, we allow for a gradient in retention along the chromosome by setting $r_{1j} = r_1$ and $r_{ij} = r_2$ $(1 < i)$, as suggested by the gradient in observed retention probabilities for these data (see Results).

For each model, and for a given locus order, breakage and retention probabilities are estimated by those values that maximize the likelihood for the radiation hybrid mapping data. Orders can be compared by their maximum likelihoods, the order with the largest maximum likelihood being best supported by the data. For a given order, models can be compared by a likelihood ratio test.

Since it is not practical to consider explicitly all $12! \approx 5 \times 10^8$ or $21! \approx 5 \times 10^{19}$ orders for the sets of 12 (Figs. 1 and 2, Table 3) or 21 loci (Figs. 4 and 5) used for RH map construction, we used a stepwise locus ordering algorithm to identify the best locus order (Boehnke *et al.,* 1991). This algorithm builds locus orders by adding one locus at a time. At each stage, it keeps under consideration those partial locus orders no more than K times less likely than the current best partial locus order. We carried out stepwise locus ordering for both the equal and the centromeric models for the 12 or 21 loci with $K = 10^{10}$.

Stepwise locus ordering results in a list of the locus orders with the largest maximum likelihoods. To construct a framework map of loci, we begin with those loci whose positions are consistent among

all locus orders with maximum likelihoods no more than 1000 times smaller than that of the best locus order. We first note whether these loci can be ordered at 1000:1. To those loci that can, we add any other loci whose best position gives a locus order maximum likelihood at least 1000 times greater than their next best position. The remaining markers are then added to the framework map one at a time to determine the possible positions for each and the relative maximum likelihood for those positions.

To integrate the information from the RH and genetic linkage mapping studies, we repeated some of the RH mapping analyses. In these repeat analyses, we considered only those locus orders in which the orientation of 6 loci agreed with their order in the 1000:1 linkage framework map. The purpose of this approach is to combine information from the 2 locus ordering methods and to achieve accurate ordering of as many loci as possible.

Fluorescence in situ hybridization (FISH). Cosmid DNA was labeled with biotin or digoxigenin either by nick-translation (Gibco-BRL) or by random priming (Boehringer Mannheim), yielding products between 200 and 400 bp. The cosmid probes were precipitated in the presence of human COT-1 DNA (Life Technologies) and preannealed for 4–6 h at 37°C. The hybridization was carried out as previously described (Edelhoff *et al.*, 1994). Biotin-labeled probes were detected with an avidin–Texas red conjugate (Boehringer Mannheim), while digoxigenin-labeled probes were detected with anti-digoxigenin–fluorescein (fluorescein isothiocyanate, FITC) conjugates (Vector, Burlingame, CA). The chromosomes were banded using Hoechst 33258-actinomycin D staining. The chromosomes and hybridization signals were visualized by fluorescence microscopy, using a dual band pass filter (Omega or Chroma, Brattleboro, VT). Each hybridization was performed a minimum of 2 times, and 20–50 cells were examined for each probe (Chang *et al.*, 1994b). Cosmids used in this study were from an arrayed chromosome 8 library constructed from flow-sorted chromosomes (Wood *et al.*, 1992; from L. L. Deaven, Los Alamos National Laboratory).

The FISH mapping data were analyzed using the Bayesian approach of Guo and colleagues (Flejter *et al.*, 1993; Guo *et al.*, 1994). In brief, this method assumes that the number of incorrect orderings for a locus pair follows a binomial distribution with error probability θ and that θ is uniformly distributed on the interval $0 \leq \theta < \frac{1}{2}$. Based on these assumptions and the observed data, we then calculate the posterior probability of correct or incorrect ordering. Since, generally, error probabilities are well less than $\frac{1}{2}$, this method tends to slightly underestimate the true posterior probability of correct ordering when the number of spreads is small.

Genetic map construction. The genetic maps were constructed with data from the CEPH families using the computer program CRI-MAP. Genotyping data were obtained from the CEPH Version 6 database for Généthon markers (Weissenbach *et al.*, 1992), from the data set described previously (Tomfohrde *et al.*, 1992), and from typing of additional CEPH families at Seattle using methods described previously (Schellenberg *et al.*, 1992b).

RESULTS

RH panel construction and marker analysis. The chromosome 8 RH panel was generated in 2 separate fusion experiments. Fusion 1 yielded 103 hybrids, and fusion 2 yielded 50 hybrids. The presence of human DNA fragments was assessed by inter-*Alu* PCR; 32 of 103 cell lines and 34 of 50 cell lines were positive for fusions 1 and 2, respectively. The RH panel was genotyped for 52 loci (Tables 1 and 2), including genes, polymorphic loci, and STSs. These markers spanned the entire chromosome. Genotypes for loci used in RH map construction were determined at least twice. Initially, all cell lines from fusion 1 (*Alu* positive and negative) were genotyped for D8S87, D8S255, D8S259, D8S268, D8S278, D8S283, and ANK1. Of the 71 *Alu*-negative cell lines, only 1 was positive for a single marker (ANK1). In subsequent experiments from fusion 1, only *Alu*-positive cell lines were used, with the exception that the single *Alu*-negative, ANK1-positive line was also included. For fusion 2, only *Alu*-positive cell lines were used for genotyping.

RH marker retention patterns. Five pairs of loci gave identical retention patterns (D8S131/APOJ, D8S339/GSR, D8S259/D8S71, D8S135/FGFR1, and D8S597/D8S598), suggesting that these markers are closely linked. For two of these pairs (D8S135/FGFR1 and D8S597/D8S598), single cosmids were identified containing both markers, confirming the close physical association of these loci. To facilitate subsequent RH map construction, genotype data from only one of each pair were used.

The observed locus retention frequencies ranged from 0.12 to 0.54 (Table 2). The retention pattern of the two fusion panels appeared quite similar. Formal tests of heterogeneity revealed no evidence for heterogeneity between the two panels (see below). Thus, for all subsequent work, data from the two panels were pooled. Markers surrounding the centromere have a higher retention frequency compared to telomeric markers. Markers spanning the centromere (GSR at 8p12 to D8S166 at 8q12, Fig. 1 and Table 2) have retention frequencies from 0.30 to 0.54, while retention frequencies for the remaining more telomeric markers range from 0.12 to 0.31. Higher retention frequencies for centromeric markers have been observed previously for several RH panels (Cox *et al.*, 1990; Ceccherini *et al.*, 1992; Gorski *et al.*, 1992; Tamari *et al.*, 1992).

Somatic cell hybrid panel. A somatic cell hybrid panel (Wagner *et al.*, 1991) was genotyped for some of the markers (Table 2). This panel can be used to resolve chromosome 8 into 9 regions designated A–I (Fig. 1). The WRN region, as defined by D8S87 and ANK1, is in region C. The panel was genotyped for 15 loci, including genes (NAT2, LHRH, and XPACII), STSs (D8S116), STRP loci (D8S598, D8S599, D8S600), and anonymous expressed sequence-tagged sites (ESTs; D8S288E, D8S289E, D8S291E, D8S292E, D8S294E, D8S295E, D8S297E, and D8S340E). Some of the other loci used in this study had been genotyped and assigned to specific regions by others (Table 2). Markers determined to be in the C region using the somatic cell hybrid panel or by FISH or colocalization of loci on a common cosmid clone (D8S135 and FGFR1) were used for subsequent RH map construction.

Multipoint analysis of RH genotype data. We focused our initial analysis on markers in the C region, close to the WRN locus (markers inclusive of and between D8S131 and ANK1, Table 2; see also Fig. 1 for a list of markers used). Both the equal and the unequal retention models gave the same best locus order. The unequal retention probability model fit the data significantly better than the equal retention probability

TABLE 1

PCR Primers for Chromosome 8 Markers

Locus	Primers (5′ to 3′)	PCR product size (bp)	Conditions ($MgCl_2$, °C)	Reference
	Genes			
Defensin 1 (DEF)	TGC AGA ATA CCA GCG TGG ATT GC AGC AAT TCC CTG TAG CTC TCA AAG C	142	3.0, 60	Daher *et al.*, 1988
Catepsins B (CTB)	AAA AGA TCT AAT CTG CCG TGG GCC CCT GCC TGA AAC TTG TAT CTT ACG T	107	1.5, 55	Chan *et al.*, 1986
N-Acetyltransferase (NAT2)	CTC TCA CTG AGG AAG AGG TTG AAG CAT CAC CAG GTT TTG GCA CGA GA	135	1.5, 55	Ohsako and Deguchi, 1990
Surfactant protein 2 (SFTP2)	GAG GAG AGC ATA GCA CCT GCA G GAG GAG GCA GGG CCA TCA CAC A	133	1.5, 60	Glasser *et al.*, 1988
Luteinizing hormone releasing hormone (LHRH)	CCT GGT GCC AAA AAG GTT GG TTG CAG TGA GCC GAG ATT GC	161	2.0, 57	
Glutathione reductase (GSR)	TTT GTC GGG CTT GGA AGT CAG CA CTC AGG TCC TTG GTA TTC GGG A	126	1.5, 65	Tutic *et al.*, 1990
Fibroblast growth factor receptor 1 (FGFR1)	GCT TTG CTG ACC AAA TGC CTG G GAT GGG TAA ATC TCT GGT AAC G	190	1.5, 58	Itoh *et al.*, 1990
	Short tandem repeats			
D8S597	GAA AAG TCT GGT TTC TGG TCC ATG AGG TAT ATA TTG TTA TCT CC	148	5.0, 55	
D8S598	CCT TTC TCA GAT GTC CTC ACG GGG CAA CAG AGC AAG ACT CC	219	2.0, 55	
D8S599	CTT TTC TCT TGG GTC TTC GTC G AAC ACA ATC TTG ACT CCA CCC	168	2.0, 55	
D8S600	CAT TTT TGT TCA AGG AGA CTG G GTT TTG ATT AAG GTC CAA GTT GC	169	2.0, 57	
D8S116	TAC CCT CTT CCT TTA GTG TGG GCA CTT ACT TGG TAG TGA AGG	230	1.5, 55	
D8S135PB	ACC TAA AAC CCT GTT CAC GAC TGA GGG GCG TTG GTA C	162	1.5, 55	
	Sequence-tagged sites			
D8S71	TGG GTA TCT CAC CAA TGA CCG TTG GTA CGC CAG AAG TGA TGC	323	1.5, 55	
D8S94	TAT CTC CTC GGA ATG AAG TTC C TTT GGA AAA TCT GAT GGC TCC C	289	1.5, 55	
D8S105	TTC CTG ATT GGA CAT TGA CTG G GCA GTA GCT CAT GTT CCA TTG G	147	1.5, 56	
D8S124	TCC AAA GGT TTA TCA CCC ATC C CTC AGG AAG GAG ACA CAT AAG C	260	1.5, 55	

Note. Primers for DEF, CTB, NAT2, SFTP2, GSR, and FGFR1 were designed from published sequences. Segments of DNA clones pL8-22, pL8-42, pBS8-91, PBS8-132, and PBS8-163 were sequenced to generate a STS for D8S71, D8S94, D8S105, D8S116, and D8S124, respectively. For LHRH, a CA-repeat track was identified in a cosmid clone containing this gene, and flanking primers were designed. The CA track was not polymorphic. For all other loci tested, published primer sequences were used: ANK1, D8S7, D8S84, D8S85, D8S87, D8S88, D8S135, D8S137, D8S164, D8S165, D8S166, D8S167, D8S198, D8S199, D8S200, D8S201, and LPL (GZ14/15) are from Tomfohrde *et al.* (1992); D8S339 is from Thomas and Drayna (1993); D8S255, D8S259, D8S268, D8S278, and D8S283 are from Weissenbach *et al.* (1992), see Genome Database (GDB), Welch Medical Library, Johns Hopkins; D8S288E, D8S289E, D8S291E, D8S292E, APOJ (D8S293E), D8S294E, D8S295E, D8S297E, and D8S340E are from Adams *et al.* (1992), see GDB; D8S131 is from Weber *et al.* (1990); D8S136 is from NIH/CEPH Collaborative Mapping Group (1992), see GDB; XPACII is from Kaur *et al.* (1992).

model ($\chi^2 = 11.35$, $df = 1$, $P < 0.0008$), consistent with our observation of decreasing retention with increasing distance from the centromere. Table 3 presents the five locus orders with maximum likelihoods no more than 1000 times less than that of the best locus order under the unequal retention model. Locus orders are presented in only their most likely orientation. The best comprehensive map under the unequal retention probability model spans 200 $cR_{10,000}$ (where 100 $cR_{10,000}$ is the distance corresponding to 1 expected radiation break per hybrid given a radiation dose of 10,000 rad) and is presented in Fig. 1, along with the distance estimates between loci, observed locus retention probabilities, and locus retention probabilities predicted by the unequal retention model. For comparison, distances estimated under the equal retention model also are provided. From these data, we constructed a framework map of 8 loci for which the markers are ordered at 1000:1 maximum likelihood ratio (Fig. 2). The additional nonframework markers could be placed in 1 of

TABLE 2

Location of Chromosome 8 Markers, Retention Frequencies (%) in RH Cell Lines, and Markers Used for Meiotic Mapping

Locus	Retention frequencies (%) in RH cell lines			Somatic cell hybrid region	Cytogenetic location (FISH)	Loci used for meiotic mapping
	1st set	2nd set	Total			
D8S201	24	24	24	A[a]		
D8S7	21	26	24	A[a]	8p23	
D8S289E	21	24	22	A[b]		
DEF	27	32	30	A[a]	8p23–p22[c]	
CTB	12	26	19		8p22[c]	
D8S599	18	29	24	B[b]		
NAT2	24	29	27	B[b]	8pter–q11[c]	
D8S297E	24	32	28	B[b]		
D8S294E	30	32	31	B[b]		
LPL	27	24	25	B[a]	8p22[c]	+
SFTP2	24	24	24	C[d]	8p[c]	
D8S136	21		21	C[a]	8p21[e]	+
LHRH	27	24	25	C[b]	8p21–p11.2[c]	
D8S137	24	24	24	C[a]	8p21[e]	+
APOJ	21	21	21		8p21–p12	
D8S131	21	18	19	C[a]	8p21[e]	+
D8S339	30	35	33			+
GSR	30	35	33	C[a]	8p12[e]	
D8S124	30	35	33	C[a]	8p23–q11	
D8S278	30	33	31			+
D8S259	33	35	34			+
D8S71	33	35	34	C[a]	8pter–q22	
D8S283	33	38	36			+
D8S87	36	42	39	C[a]	8p12[e]	+
D8S105	33	35	34	C[a]	8p23–q11	
FGFR1	30		30		8p12[c]	+
D8S135	30	44	37	C[a]	8p11.2[e]	
D8S135PB	36		36			
D8S255	44	50	46			+
ANK1	45	44	45	C[a]	8p11.2[e]	+
D8S268	52	47	49	C[a]		+
D8S291E	42	41	42	C[b]		
D8S94	52	53	52	C[a]		
D8S292E	52	56	54	C[b]		
D8S165	36	32	34	E[a]		
D8S166	33	32	33	E[a]		
D8S288E	27	29	28	F[b]		
D8S164	18	32	27	F[a]		
D8S84	18	35	28	F[a]	8q13–q21.2	
D8S340E	15	18	16	F[b]		
D8S167	21	12	16	G[a]		
D8S88	27	15	21	G[a]		
D8S600	18	15	16	H[b]		
D8S295E	18	24	21	I[b]		
D8S200	24	21	22	I[a]		
D8S85	30	21	26	I[a]	8q21–q22	
D8S116	18	20	19	I[b]	8p23–q11	
D8S597	21		21			
D8S598	21	29	25	I[b]		
D8S199	18	24	21	I[a]		
D8S198	12	21	16	I[a]		
XPACII	9	15	12			

Note. Markers are listed in the approximate order in which they occur, starting with the telomeric region of 8p and extending to the telomeric region of 8q.

[a] From Wagner *et al.* (1991) and Tomfohrde *et al.* (1992).

[b] Location determined as part of this study by PCR analysis of a somatic cell hybrid panel (Wagner *et al.*, 1991).

[c] From Sparkes *et al.* (1989) (DEF), Fong *et al.* (1992) (CTB), Blum *et al.* (1990) (NAT2), Mattei *et al.* (1993) (LPL), Fisher *et al.* (1988) (SFTP2), Williamson *et al.* (1991) (LHRH), and Ruta *et al.* (1989) (FGFR1). The locations of the other markers were taken from GDB.

[d] Westbrook *et al.* (1993).

[e] Determined by FISH analysis.

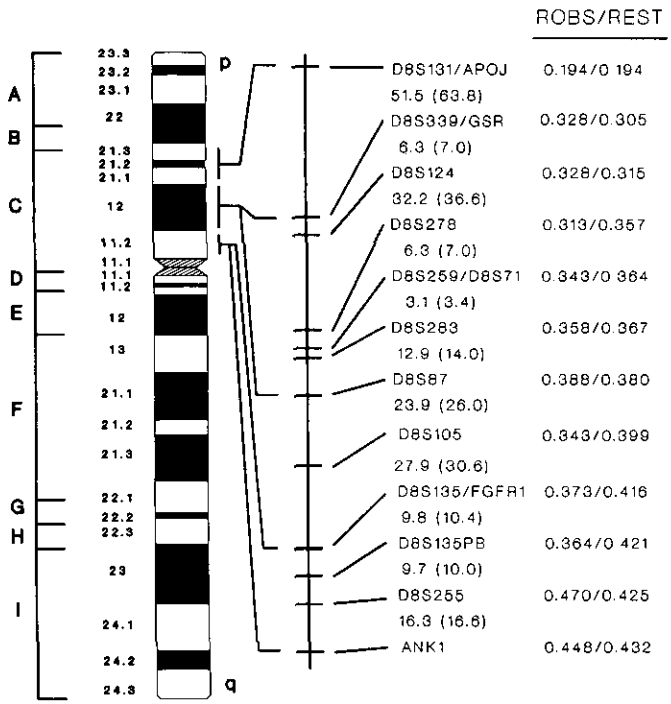

FIG. 1. Chromosome 8 and a comprehensive RH map of WRN region. The letters A–I are regions defined by the somatic cell hybrid panel described by Wagner *et al.* (1991). Numbers between loci indicate the distances in $cR_{10,000}$ for the unequal retention model, with distances under the equal retention model given in parentheses. The righthand-most column gives observed locus retention probabilities (ROBS) and estimated locus retention probabilities for the unequal retention model (REST).

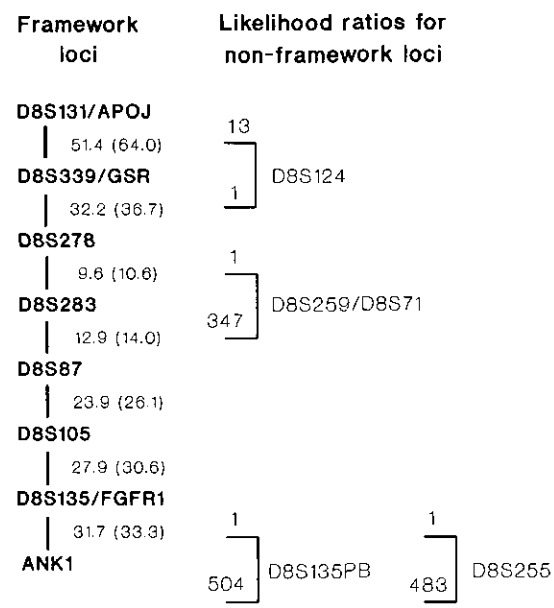

FIG. 2. Framework RH map of the WRN region. The framework map for the unequal retention method is given in the center column with distances in $cR_{10,000}$ given between each marker; distances under the equal retention model are given in parentheses. Likelihood ratios of at least 1000:1 support the framework order shown. For nonframework markers, potential intervals are given on the right side of the figure; 1 indicates the most likely interval, and the second value for a marker indicates likelihood ratios against localization in a given interval.

2 intervals. The framework map had a total length of 190 $cR_{10,000}$. The difference in map length between the comprehensive and framework maps suggests that there may be some inflation of map length due to errors in the genotyping data.

RH map construction was also attempted using all of the markers listed in Table 2. However, the loci order obtained was grossly inconsistent with regional localizations obtained with the somatic cell hybrid panel and with other mapping techniques. The inability to order the entire marker set was due to the combined effects of the large spacing of markers outside of the WRN region and the limited number of hybrid cell lines available.

Genetic analysis of chromosome 8 markers. A genetic linkage map of the WRN region was constructed using data from 13 STRP (Table 2) loci. Markers used included loci from 2 previously published, independent genetic maps (Weissenbach *et al.*, 1992; Tomfohrde *et al.*, 1992), and new STRP markers not previously mapped (D8S131 and FGFR1, Yu *et al.*, 1994a,b; D8S339, Thomas and Drayna, 1993). FGFR1 was used in place of D8S135 since the former is substantially more polymorphic and both are present on the same cosmid. Additional families were also genotyped for Généthon markers D8S283, D8S259, and D8S278 (Weissenbach *et al.*, 1992). The resulting female, sex-equal, and male maps are presented in Fig. 3 and maximum likelihood ratios supporting these orders are given in Table 4. The following markers could not be unambiguously ordered by linkage analysis because no recombinants were observed between them (Table 4): D8S131 and D8S137; D8S87, D8S278, D8S259, and

TABLE 3

Locus Order for WRN Region Loci Assuming Unequal Marker Retention

Rank	Likelihood ratio	Locus order											
1	1	D8S131	D8S339	D8S124	D8S278	D8S259	D8S283	D8S87	D8S105	D8S135	D8S135PB	D8S255	ANK1
2	13	D8S131	D8S124	D8S339	D8S278	D8S259	D8S283	D8S87	D8S105	D8S135	D8S135PB	D8S255	ANK1
3	347	D8S131	D8S339	D8S124	D8S278	D8S283	D8S259	D8S87	D8S105	D8S135	D8S135PB	D8S255	ANK1
4	957	D8S131	D8S339	D8S124	D8S278	D8S259	D8S283	D8S87	D8S105	D8S135	D8S135PB	ANK1	D8S255
5	988	D8S131	D8S339	D8S124	D8S278	D8S259	D8S283	D8S87	D8S105	D8S135	D8S255	ANK1	D8S135PB

Note. Underlined loci are in a different order compared to the most likely order.

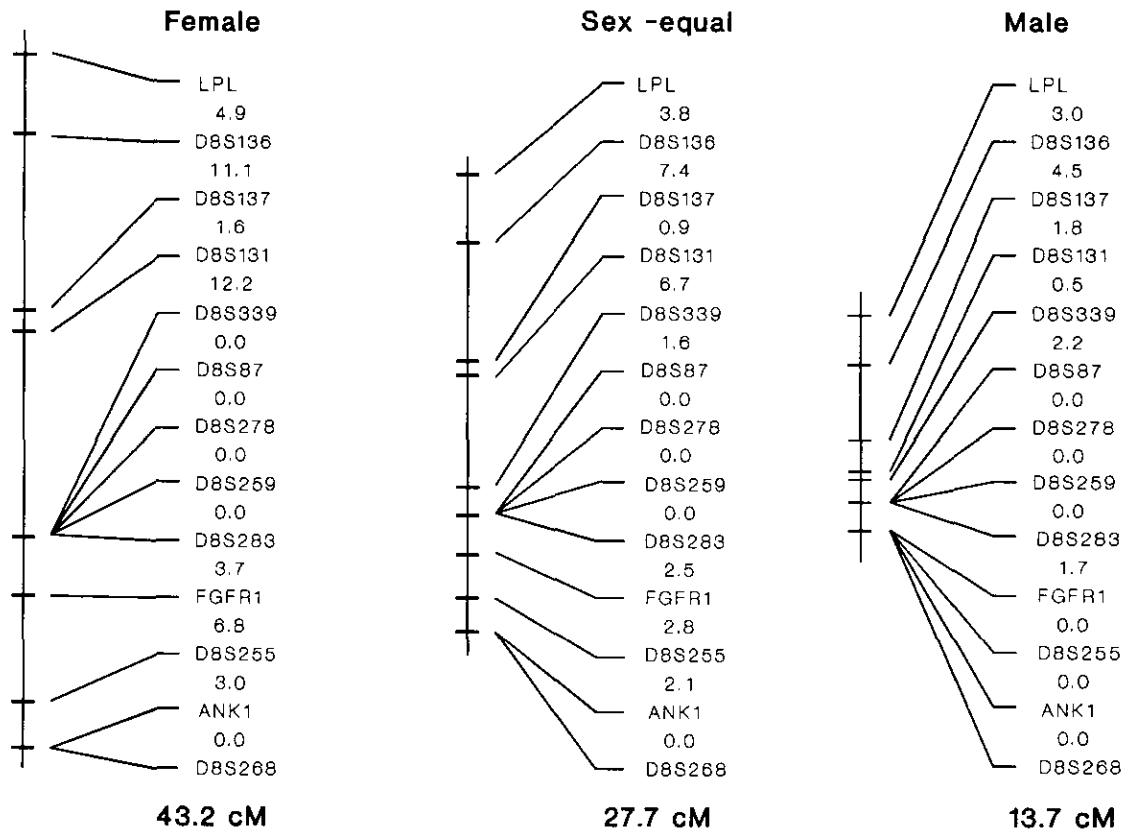

FIG. 3. Comprehensive genetic maps of the WRN region. Male, sex-equal, and female genetic maps are presented along with the total distances for each map. Distances between markers are given in cM and were computed with the Kosombi interference function. Genotypes for GZ14/15, LPL5GT, and LPL3GT, which are 3 different STRP loci at the LPL locus (Tomfohrde *et al.*, 1992), were haplotyped. The map presented is the best order and is not a framework map since for some markers, the computed odds supporting inversion of adjacent markers were not 1000:1 for all loci (Table 4).

D8S283; ANK1 and D8S268. However, by examining crossovers, D8S137/D8S131 could be located between D8S136 and D8S339, and ANK1/D8S268 proximal to D8S255. Also, in the center of the map, D8S87/D8S278/D8S283 could be placed between D8S339 and FGFR1 on the basis of at least 1 clear crossover event, and similarly D8S259 could be placed between D8S131/D8S137 and FGFR1.

FISH analysis of chromosome 8 markers. To confirm further the locus order obtained from RH mapping and to anchor the RH map to specific chromosome 8 bands, FISH analysis of some loci was performed. Seven loci corresponding to 2 genes (ANK1 and GSR), and 5 STRP loci (D8S87, D8S131, D8S136, D8S137, D8S133) were mapped by FISH to a region spanning from the centromere to band 8p22. In addition, D8S135 and DNA polymerase β had been previously mapped by the same method (Chang *et al.*, 1994b). ANK1, D8S135, and DNA polymerase β mapped to 8p11.2, D8S87 and GSR to 8p12, D8S131, D8S136 and D8S137 to 8p21, and D8S133 to 8p21.3–p22 (Fig. 1). In each hybridization, at least 20 metaphase cells were analyzed, showing signals on one or both chromatids at the assigned site in 80–90% of the examined cells.

Two-color FISH was used to establish the order of D8S87, GSR, and D8S131. Pairs of cosmids corresponding to these loci were labeled with biotin or digoxigenin, so that in each paired hybridization, red and green signals could be identified (Table 5). Three separate experiments were performed: D8S87 was hybridized to metaphase chromosomes together with GSR, GSR with D8S131, and D8S87 with D8S131. The relative order of the hybridization signals for D8S131 with GSR, D8S131 with D8S87, and GSR with D8S87 was scored as being distal, even, or proximal (Table 5). The 3 experiments together indicate the order centromere–D8S87–GSR–D8S131–telomere, consistent with the RH and genetic mapping results. Furthermore, the data suggest distances of greater than 1–2 Mb between D8S131, GSR, and D8S87, since most chromatids showed distinct signals and a consistent relative order of the signals (Trask *et al.*, 1991, 1994; Lawrence *et al.*, 1990). Analysis of the 3 FISH experiments (Flejter *et al.*, 1993; Guo *et al.*, 1994) resulted in posterior probabilities of incorrect ordering of less than 10^{-6} for each experiment, suggesting very high confidence in the overall 3-point locus order inferred.

Map integration. We also attempted to construct a RH map for all of the C region markers and LPL (region B). When RH genotypes for 21 markers spanning this region (Fig. 1, Tables 2 and 6; markers used are shown in Figs. 4 and 5) were analyzed under the unequal

TABLE 4

Meiotic Mapping Analysis

Marker	Odds against flipping adjacent markers ($\log_{10}$ odds)[a]	Number of crossovers between adjacent markers[b]	Lod scores between adjacent markers $[Z(\theta_f, \theta_m, \theta_{ave})]$[c]
LPL			
	5.3	6	34.2 (0.05, 0.03, 0.04)
D8S136			
	18.9	7	24.3 (0.07, 0.04, 0.06)
D8S137			
	0.0	0	8.4 (0.00, 0.00, 0.00)
D8S131			
	3.8	2	7.6 (0.17, 0.00, 0.03)
D8S339			
	3.1	1	18.8 (0.00, 0.03, 0.01)
D8S87			
	0.0	0	13.2 (0.00, 0.00, 0.00)
D8S278			
	0.0	0	13.2 (0.00, 0.00, 0.00)
D8S259			
	0.0	0	19.3 (0.00, 0.00, 0.00)
D8S283			
	10.7	3	14.9 (0.10, 0.02, 0.04)
FGFR1			
	5.7	2	23.2 (0.06, 0.00, 0.02)
D8S255			
	3.4	1	16.3 (0.02, 0.00, 0.02)
ANK1			
	0.0	0	15.4 (0.00, 0.00, 0.00)
D8S268			

[a] Sex-specific analysis using flips option of CRIMAP.
[b] Determined using CRIMAP chrompic routine.
[c] Pairwise sex-specific maximum lod scores. In parentheses the maximum likelihood estimates for recombination frequencies are listed for female, male, and sex-pooled meioses, respectively.

retention model, 46 locus orders had a maximum likelihood no more than 1000 times less than that of the best locus order, and 11 loci could be placed in a 1000:1 framework map (Fig. 4B). However, the positions of several markers at the end of the map were not well defined. For example, D8S136 and LPL could be placed at either end. A comprehensive RH map spanning 514.7 $cR_{10,000}$ and a framework RH map for these 21 loci are given in Figs. 4A and 4B, respectively. Distance estimates under the equal retention model also are provided for comparison; this model again fit the data less well than the unequal model ($\chi^2 = 15.11$, $df = 1$, $P < 0.0002$).

TABLE 5

Order of D8S131, GSR, and D8S87 by Two-Color FISH

	Locus (band)		
Locus	D8S131 (8p21)	GSR (8p12)	D8S87 (8p12)
D8S131	—	38:6:2[a]	47:1:1
GSR	—	—	23:2:0

[a] The number of chromatids in which the hybridization signals of the probes listed in columns are distal, even, or proximal, respectively, to the loci listed across the top.

To facilitate the ordering of a larger number of loci, results from meiotic mapping (Table 4 and Tomfohrde *et al.*, 1992) were used to impose the marker order LPL–D8S137–D8S87–FGFR1–ANK1 for 6 loci in the WRN region. The order for these 6 loci was supported at 1000:1 relative maximum likelihood in the meiotic mapping analysis. When the RH data were reanalyzed under the constraint that these 6 loci be so ordered, the same comprehensive map was obtained as before (Fig. 4A), and a new framework map of 13 loci was obtained (Fig. 5). The new framework map was consistent with the unrestrained framework map of 11 loci, and the positions of the nonframework markers were in several cases more clearly specified. Under the constraint, all 21-loci orders within 1000:1 maximum likelihood were consistent with the ordering (D8S292E, D8S94, D8S291E)–(D8S268, ANK1)–D8S255–D8S135PB–D8S135–D8S105–D8S87–(D8S283, D8S259)–D8S278–(D8S124, D8S339)–D8S131–D8S137–LHRH–(D8S136, SFTP2, LPL), where loci within parentheses were not convincingly ordered among themselves. However, since LPL is in the B-region and SFTP2 and D8S136 are in the C-region as determined by data from the somatic cell hybrid panel (Fig. 1 and Table 2), LPL can be considered the most telomeric of the loci in this group.

TABLE 6

Marker Retention Patterns for the WRN Region

Hybrid number	Hybrid name	Number observed	Obligate breaks	Locus order																				
				D8S292E	D8S94	D8S291E	D8S268	ANK1	D8S255	D8S1351PB	D8S1351	D8S1051	D8S87	D8S823	D8S259	D8S278	D8S1243	D8S339	D8S131	D8S137	LHRH	D8S1136	SFTP2	LPL
1	06D2	1	0	–	–	–	–	–	0	–	–	–	–	–	–	–	–	–	–	–	–	–	–	–
2	10D1	1	0	–	–	–	–	–	–	–	–	–	–	–	–	–	–	–	–	–	–	–	–	–
3	11A4	1	1	+	+	+	+	–	–	–	–	–	–	–	–	–	–	–	–	–	–	–	–	–
4	18E3	1	2	–	–	–	+	–	–	–	–	–	–	–	–	–	–	–	–	–	–	–	–	–
5	22D1	1	3	–	–	–	–	–	–	–	–	–	+	+	+	+	+	+	+	+	+	–	–	+
6	24C5	1	5	+	+	–	+	+	+	+	–	–	–	–	–	–	–	–	+	+	+	–	–	–
7	33D4	1	3	+	+	–	+	+	+	+	–	–	–	–	–	–	–	–	–	–	–	–	–	–
8	52E4	1	4	+	+	+	+	+	+	–	–	–	+	+	+	+	+	+	–	–	–	–	–	+
9	01A1	1	2	+	+	+	+	+	+	+	+	+	+	+	+	+	+	+	–	–	–	+	+	+
10	01C1	1	0	–	–	–	–	–	–	–	–	–	–	–	–	–	–	–	–	–	–	–	–	–
11	01C7	1	0	–	–	–	–	–	–	–	–	–	–	–	–	–	–	–	–	–	–	–	–	–
12	01E4	1	2	+	+	+	+	+	+	–	–	–	–	–	–	–	–	–	–	–	–	+	+	+
13	03B2	1	1	+	+	+	+	+	+	+	+	+	+	+	+	+	–	–	–	–	–	–	–	–
14	16C5	1	3	–	–	–	–	–	–	–	–	+	–	–	–	–	–	–	–	–	+	+	+	+
15	17C6	1	0	–	–	–	–	–	–	–	–	–	–	–	–	–	–	–	–	–	–	–	–	–
16	21A5	1	0	–	–	–	–	–	–	–	–	–	–	–	–	–	–	–	–	–	–	–	–	–
17	23B5	1	3	–	–	–	+	+	+	+	+	+	+	+	+	+	+	+	+	+	–	+	+	
18	24D6	1	1	+	+	+	–	–	–	–	–	–	–	–	–	–	–	–	–	–	–	–	–	–
19	25D2	1	2	+	+	+	+	+	+	+	+	–	–	–	–	–	–	–	–	–	–	–	–	+
20	27C2	1	0	+	+	+	+	+	+	+	+	+	+	+	+	+	+	+	+	+	+	+	+	+
21	31A2	1	5	+	+	–	+	+	+	+	+	+	+	–	–	–	–	–	–	+	–	–	–	–
22	35B2	1	3	+	+	+	–	–	–	–	–	–	–	–	–	–	–	–	–	–	–	–	+	–
23	38A3	1	0	–	–	–	–	–	–	–	–	–	–	–	–	–	–	–	–	–	–	–	–	–
24	44A6	1	1	–	–	–	–	–	–	–	–	–	–	–	–	–	–	–	–	+	+	+	+	
25	47B3	1	1	+	+	+	+	+	+	+	+	+	+	+	+	+	+	+	+	–	–	–	–	
26	49E1	1	3	+	+	+	+	–	–	–	–	–	–	–	–	–	–	+	+	+	+	+	–	
27	49E3	1	0	–	–	–	–	–	–	–	–	–	–	–	–	–	–	–	–	–	–	–	–	–
28	51C6	1	2	–	–	–	–	–	–	–	–	+	+	+	+	+	+	+	–	–	–	–	–	–
29	53C1	1	5	+	+	+	+	+	+	+	+	+	+	+	+	–	+	–	–	–	+	+	–	–
30	53E1	1	1	+	+	+	+	+	+	+	+	+	+	+	+	+	+	–	–	–	–	–	–	–
31	56A5	1	0	–	–	–	–	–	–	–	–	–	–	–	–	–	–	–	–	–	–	–	–	–
32	56E2	1	1	+	+	+	+	+	+	+	+	+	+	+	+	+	+	+	+	+	+	–	–	–
33	02E2	1	2	–	–	–	–	+	–	–	–	–	–	–	–	–	–	–	–	–	–	–	–	–
34	F02G	1	0	–	–	–	–	–	–	0	–	–	–	–	–	–	–	–	–	–	–	0	–	–
35	F06E	1	3	–	–	–	+	+	+	0	+	–	–	–	–	–	–	–	–	–	–	0	–	+
36	F13C	1	1	+	+	+	+	+	+	0	+	+	+	+	+	+	–	–	–	–	–	0	–	–
37	F13E	1	5	–	–	–	–	–	+	0	+	–	+	+	+	+	+	+	–	–	–	0	+	+
38	F16B	1	0	+	+	+	+	+	+	0	+	+	+	+	+	+	+	+	+	+	+	0	+	+
39	F22H	1	5	+	+	–	+	+	+	0	+	–	–	+	+	+	+	+	–	–	–	0	–	–
40	F23A	1	0	–	–	–	–	–	–	0	–	–	–	–	–	–	–	–	–	–	–	0	–	–
41	F24C	1	5	–	–	–	–	–	–	0	–	–	+	–	–	–	–	–	–	+	–	0	–	+
42	F25D	1	0	–	–	–	–	–	–	0	–	–	–	–	–	–	–	–	–	–	–	0	–	–
43	F25E	1	1	+	+	–	–	–	–	0	–	–	–	–	–	–	–	–	–	–	–	0	–	–
44	F26H	1	3	+	+	+	+	+	+	0	+	+	+	+	+	+	–	–	+	+	–	0	–	–
45	F27H	1	1	+	+	+	+	+	+	0	+	+	+	+	+	+	+	+	–	–	–	0	–	–
46	F29B	1	3	+	+	+	+	+	+	0	+	+	+	+	+	+	+	+	–	–	–	0	+	–
47	F29G	1	1	–	–	–	–	–	–	0	–	–	–	–	–	–	–	–	–	–	+	0	+	+
48	F31B	1	1	+	+	+	+	+	+	0	+	+	+	+	+	–	–	–	–	–	–	0	–	–
49	F31F	1	0	–	–	–	–	–	–	0	–	–	–	–	–	–	–	–	–	–	–	0	–	–
50	F34F	1	4	–	–	–	–	–	–	0	–	–	–	–	–	–	+	+	–	–	+	0	–	–
51	F36B	1	2	–	–	–	–	–	–	0	–	–	–	–	–	–	+	+	–	–	–	0	–	–
52	F37B	1	1	+	+	+	+	+	–	0	–	–	–	–	–	–	–	–	–	–	–	0	–	–
53	F38A	1	0	–	–	–	–	–	–	0	–	–	–	–	–	–	–	–	–	–	–	0	–	–
54	F38E	1	1	+	+	–	–	–	–	0	–	–	–	–	–	–	–	–	–	–	–	0	–	–
55	F40H	1	1	+	+	+	+	+	+	0	+	+	+	+	+	+	–	–	–	–	–	0	–	–
56	F41B	1	2	+	+	–	–	–	–	0	–	–	–	–	–	–	+	+	+	+	+	0	+	+
57	F41C	1	1	+	–	–	–	–	–	0	–	–	–	–	–	–	–	–	–	–	–	0	–	–

TABLE 6—*Continued*

Hybrid number	Hybrid name	Number observed	Obligate breaks	Locus order																				
				D8S292E	D8S94	D8S291E	D8S268	ANK1	D8S255	D8S135PB	D8S135/FGFR1	D8S105	D8S87	D8S283	D8S259	D8S278	D8S124	D8S339/GSR	D8S131/APOJ	D8S137	D8S136	LHRH	SFTP2	LPL
58	F42C	1	5	−	−	−	+	−	+	0	+	+	+	+	+	+	+	+	−	−	+	0	+	+
59	F42F	1	1	+	+	+	+	+	+	0	+	−	−	−	−	−	−	−	−	−	−	0	−	−
60	F42G	1	3	+	+	+	+	+	+	0	+	+	−	−	−	−	+	+	+	+	+	0	+	−
61	F43G	1	3	+	+	+	−	−	−	0	−	+	+	+	−	−	−	−	−	−	−	0	−	−
62	F44F	1	0	−	−	−	−	−	−	0	−	−	−	−	−	−	−	−	−	−	−	0	−	−
63	F47B	1	1	+	+	+	+	+	+	0	+	+	+	+	+	+	+	+	+	+	+	0	−	−
64	F47H	1	3	+	+	+	+	+	+	0	−	−	−	−	−	−	−	−	−	+	+	0	−	−
65	F53C	1	2	−	−	−	−	−	+	0	−	−	−	−	−	−	−	−	−	−	−	0	−	−
66	F53F	1	2	−	−	−	−	−	−	0	−	−	+	−	−	−	−	−	−	−	−	0	−	−
67	F55H	1	2	+	+	+	+	+	+	0	+	+	+	+	+	+	+	+	+	+	−	0	+	+

Note. +, scores; −, absent; 0, not genotyped. Genotyping data for APOJ, GSR, and D8S71 are not shown. Hybrids beginning with the letter "F" are from the second fusion hybrid panel.

Two markers included in the 1000:1 framework map (Fig. 4B) were not included as framework markers in the integrated map (Fig. 5). D8S131 is placed at the end of the RH framework map, but in the integrated map, it falls in 1 of 2 very large gaps between D8S136 and D8S137 and between D8S137 and D8S339/GSR.

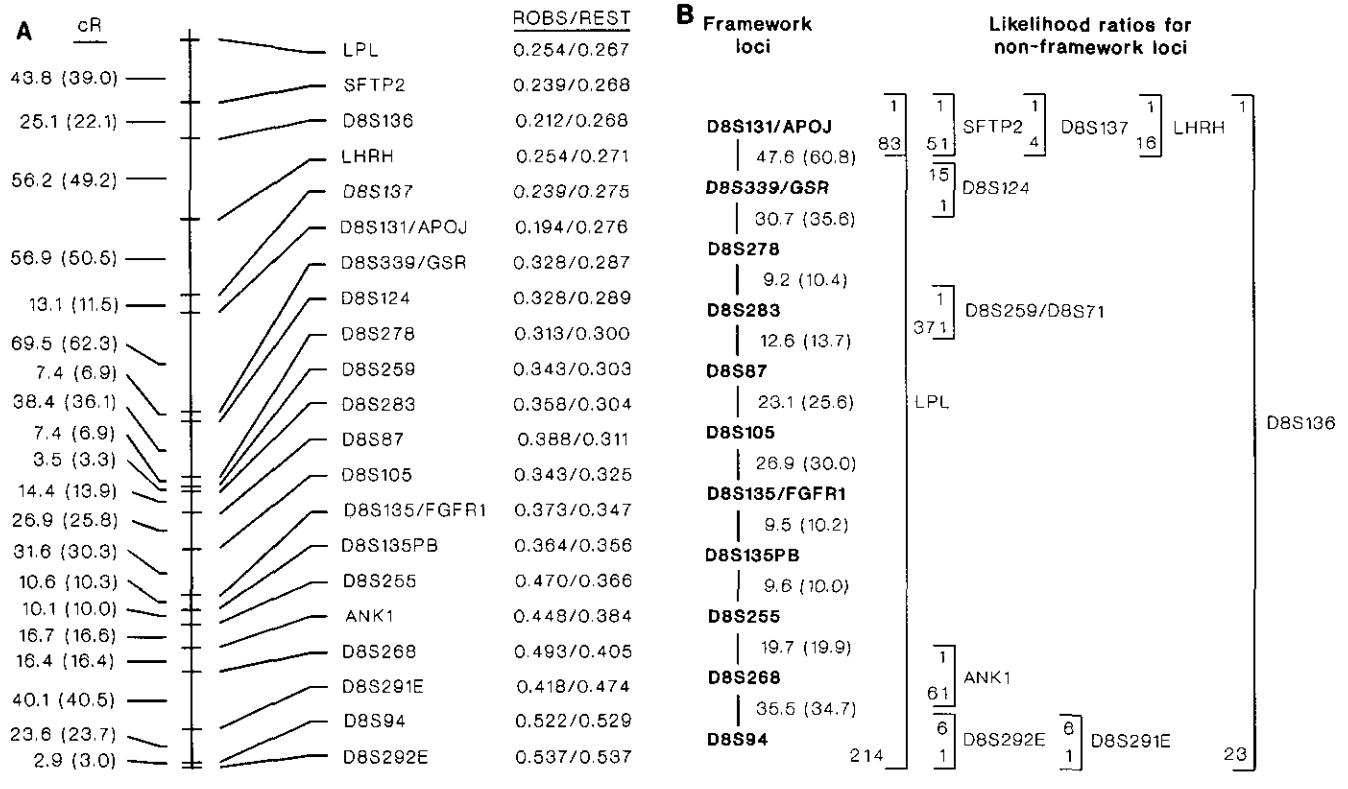

FIG. 4. Comprehensive and framework map of 21 C-region loci. (**A**) Comprehensive RH map. Numbers in the lefthand column are distances in $cR_{10,000}$ under the unequal retention model, with distances under the equal retention model given in parentheses. The righthand-most column gives observed locus retention probabilities (ROBS) and estimated locus retention probabilities for the unequal retention model (REST). (**B**) Framework map. Likelihood ratios of at least 1000:1 support the framework order shown. Numbers between markers are distances in $cR_{10,000}$ under the unequal retention model, with distances under the equal retention model given in parentheses. For nonframework markers, potential intervals are given on the right side of the figure; 1 indicates the most likely interval and the second value for a marker indicates likelihood ratios against localization in a given interval.

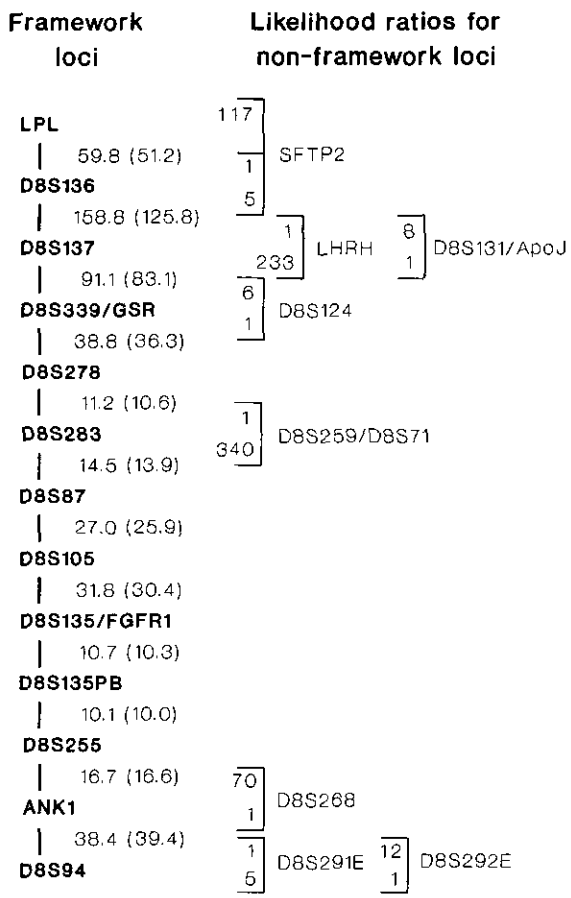

FIG. 5. Integrated map of WRN region. The integrated RH map was constructed assuming the unequal retention model and the following forced locus order: LPL–D8S136–D8S137–D8S87–D8S135(FGFR)–ANK1. Map distances and likelihood ratio annotations are as described in Fig. 4.

Given the large size of these gaps (158.8 and 91.1 cR, respectively), specific placement within them is uncertain, so that D8S131 cannot be placed confidently in the integrated framework map. D8S268 also is included in the RH framework map but not the integrated map. In this case, it is because either D8S268 or the nearby marker ANK1, but not both, can be placed with confidence in the framework map. Since ANK1 was forced into the integrated map, D8S268 could not be included.

DISCUSSION

A RH panel for chromosome 8 was generated and used to construct a RH map of the WRN region. When 15 loci spanning 8p11.2–p12 were used, a map spanning 200 cR was obtained (Table 3, Fig. 1). Of the 15 markers, 3 pairs could not be resolved because identical retention patterns within each pair were observed. Because no obligate breaks were detected between each pair, the identical retention patterns suggest that the markers within a pair are closely adjacent loci. The close physical proximity was confirmed for D8S135/FGFR1 as both markers were found in the same cosmid, indicating a maximum distance of 40 kb. The RH marker order obtained was consistent with results from genetic mapping (Tomfohrde *et al.*, 1992; Weissenbach *et al.*, 1992; Fig. 3). In particular, previous genetic mapping yielded the order D8S131–D8S87–D8S135–ANK1, which is the same as that obtained by RH analysis. In addition, the polymorphic markers D8S278 and D8S283, which could not be genetically ordered due to a lack of recombinants (Weissenbach *et al.*, 1992), could be resolved by RH analysis. Also, several genes (FGFR1, GSR, and APOJ) and nonpolymorphic STSs (D8S124, D8S105) could be located relative to polymorphic loci. Further, the RH mapping results are consistent with the limited FISH information for ordering D8S131, GSR, and D8S87. The agreement of the RH map with data from other mapping methods indicates that this RH panel will be useful for developing a higher resolution map of the region.

All analyses described above made use of 2 separate radiation hybrid panels (see Materials and Methods). As noted previously, retention frequencies for the various markers were quite similar in the 2 panels (Table 2). In addition, we carried out a large sample heterogeneity test under the best locus order for those 19 of the 21 analyzed region C markers that were genotyped in both panels. For this test, the sum of the maximum log-likelihoods for the best locus order for each panel separately was compared to the maximum log-likelihoods for the best locus order for the combined panel. The resulting χ^2 heterogeneity test statistic did not approach statistical significance ($\chi^2 = 17.81$, $df = 20$, $P = 0.60$), providing further evidence that pooling results for the 2 panels was appropriate.

The genetic map constructed contains 3 new STRP markers not previously genetically mapped (Fig. 3). These are FGFR1, D8S131 (formerly mapped as an RFLP polymorphism), and D8S339. Note that FGFR1 localized to the interval between the D8S87/D8S283/D8S278 cluster and ANK1 at greater than 1000:1 odds (Table 4). Previously, the only marker in this region was D8S135, which could not be unambiguously assigned to the same interval. The male and female maps differ substantially in length, with the female map being over 3 times as long as the male map. χ^2 analysis indicates that the overall length difference is significant at the $P < 0.01$ level, although length differences for individual intervals were not significantly different ($P > 0.05$). The higher female recombination rates appear to occur across the entire length of the region mapped. The region between D8S339 and D8S136 remains poorly mapped. Not only are there relatively large gaps in this region (6.7 cM between D8S339 and D8S131 and 7.4 cM between D8S137 and D8S136, sex-averaged distance), but also the markers in this region (D8S131 and D8S137) cannot be unambiguously ordered by either genetic or RH mapping (Fig. 4). It may be possible to resolve the order of D8S137 and D8S131 by genotyping the complete CEPH family panel. However, additional markers are clearly needed in this region.

The integrated map presented in Fig. 5 combines information from both genetic and RH mapping. The genetic framework markers (those ordered at greater than 1000:1 odds of inversion) were used to force an order for the analysis of the RH genotyping data. The resulting map yielded significantly more information than either the RH or the genetic maps alone. For example, the integrated framework map (Fig. 5) contained 2 more loci compared to the standard RH map generated for the same markers (Fig. 4B). Also, for markers D8S136 and LHRH, which could not be ordered at greater than 1000:1 odds, the integrated map method yielded less ambiguous locations with 2 potential intervals indicated (Fig. 5) rather than possible locations at either end of the map (Fig. 4B). Also, genetic mapping could not resolve the cluster D8S278, D8S259, D8S283, and D8S87, while both the standard RH maps (Figs. 2 and 4B) and the integrated map (Fig. 5) could unambiguously order 3 of these 4 markers. Because genotyping a RH panel for a marker requires less time than genotyping STRP loci for genetic analysis, the integrated mapping is a very cost-effective approach for adding a large number of new markers to existing genetic maps. Since for RH mapping markers do not need to be polymorphic, newly identified genes including anonymous EST sites (e.g., D8S291E and D8S292E) and STS markers, such as D8S124, D8S105, and D8S94, can be rapidly incorporated into the combined map. Localization of nonpolymorphic loci can provide a starting point for identifying additional polymorphic markers to fill in gaps in the genetic map. Also, mapping of ESTs such as D8S282E and D8S291E and genes SFTP2, LHRH, FGFR1, APOJ, and GSR relative to known genetic markers permits the rapid evaluation of these expressed sequences as potential candidates for the WRN gene. However, some expressed sequences could not be mapped on the RH panel by PCR-based methods because PCR amplification produced similar signal products from both human and hamster DNA. Presumably the corresponding hamster gene was sufficiently homologous to the human gene so that primer annealing and amplification could occur from both genomes. In other cases, PCR primer sets designed from cDNA sequences did not produce products, presumably because either the primer sequence was interrupted by an intron/exon boundary or because lengthy intron sequences separated the primers. These complications prevented localization of EGR3, NEFL, PLAT, D8S290E, and D8S296E.

The strategy that we used to map integration was to fix the order of loci ordered at 1000:1 in the linkage analysis in the subsequent RH mapping. This strategy has the advantage of combining information from the 2 mapping methods, permitting accurate ordering of more of the typed markers. However, it should be noted that such strategy is approximate rather than exact; even loci ordered at 1000:1 can in principle be ordered incorrectly. The best strategy for map integration would be the simultaneous analysis of the RH and linkage mapping data. Such a strategy, while theoretically possible, cannot yet be carried out with available software. Since it is likely that loci mapped at 1000:1 are ordered correctly, it is very unlikely that the approximate and exact methods would yield different maps.

Our RH, genetic, and integrated map will facilitate the fine-mapping of the WRN locus. Initial analysis of the WRN region, using 2-point and multipoint linkage methods, indicated that WRN was between ANK1 and D8S87, although a location on either side of ANK1/D8S87 could not be excluded (Goto *et al.*, 1992). Haplotype analysis of affected subjects from consanguineous matings also suggested that WRN was between D8S87 and ANK1 (Goto *et al.*, 1992). Analysis of an independent set of WS families (Schellenberg *et al.*, 1992a; Nakura *et al.*, 1993) was consistent with the WRN locus being in the vicinity of D8S87 and ANK1. Subsequent work identified a new marker, D8S339, for which fewer recombinants in WS families were observed. This marker was thought to be closer to the WRN locus than either D8S87 or ANK1 (Thomas *et al.*, 1993). Again, haplotype analysis of WS families suggested that D8S339 was between D8S87 and ANK1 (Thomas *et al.*, 1993). However, the genetic, RH, and FISH results presented here suggest that D8S339 is telomeric to both D8S87 and ANK1, suggesting that the WRN locus may be in the interval between D8S87 and D8S131. In light of the maps presented here, the localization of the WRN locus needs to be reevaluated.

ACKNOWLEDGMENTS

Supported by NIA grant R01-AG08303 (G.M.M.), NCHGR grants *HG00835* (J.L.W.), *HG00209* (M.B.), and *HG00172* (M.J.W., D.E.W.), MRC grant MT-12194 (S.W.) and a grant from the Deutsche Forschungsgemeinschaft, Germany (S.E.). We thank Matt Stephenson for computer assistance for the genetic mapping studies, Barbara J. Trask for helpful advice and discussion, and Charles E. Ogborn for assistance in cell culture.

REFERENCES

Adams, M. D., Dubnick, M., Kerlavage, A. R., Moreno, R., Kelly, J. M., Utterback, T. R., Nagle, J. W., Fields, C., and Venter, J. C. (1992). Sequence identification of 2,375 human brain genes. *Nature* **355:** 632–634.

Ben Othamane, K., Ben Hamida, M., Hentati, F., Lennon, F., Ben Hamida, C., Blel, S., Roses, A. D., Pericak-Vance, M. A., and Vance, J. M. (1993). Autosomal recessive Charcot–Marie–Tooth disease type A: Evidence of genetic linkage of CMT4 to chromosome 8q. *Cytogenet. Cell Genet.* **64:** 142.

Blanton, S. H., Heckenlively, J. R., Cottingham, A. W., Friedman, J., Sadler, L. A., Wagner, M., Friedman, L. H., and Daiger, S. P. (1991). Linkage mapping of autosomal dominant retinitis pigmentosa (RP1) to the pericentric region of human chromosome 8. *Genomics* **11:** 857–869.

Blum, M., Grant, D. M., McBride, W., Heim, M., and Meyer, U. A. (1990). Human arylamine *N*-acetyltransferase genes: Isolation, chromosomal localization, and functional expression. *DNA Cell. Biol.* **9:** 193–203.

Boehnke, M., Lange, K., and Cox, D. R. (1991). Statistical methods for multipoint radiation mapping. *Am. J. Hum. Genet.* **49:** 1174–1188.

Ceccherini, I., Romeo, G., Lawrence, S., Breuning, M. H., Harris, P. C., Himmelbauer, H., Frischauf, A. M., Sutherland, G. R., Germino, G. G., Reeders, S. T., and Morton, N. E. (1992). Construction of a map of chromosome 16 by using radiation hybrids. *Proc. Natl. Acad. Sci. USA* **89:** 104–108.

Chan, S. J., Segundo, B. S., McCormick, M. B., and Steiner, D. F. (1986). Nucleotide and predicted amino acid sequences of cloned human and mouse preprocatepsin B cDNA. *Proc. Natl. Acad. Sci. USA* **83:** 7721–7725.

Chang, M., Tsuchiya, K., Batchelor, R. H., Rabinovitch, P. S., Kulander, B. G., Haggitt, R. C., and Burmer, G. C. (1994a). Deletion mapping of chromosome 8p in colorectal carcinoma and dysplasia arising in ulcerative colitis, prostatic carcinoma, and malignant fibrous histiocytomas. *Am. J. Pathol.* **144:** 1–6.

Chang, M., Burmer, G. C., Sweasy, J., Loeb, L. A., Edelhoff, S., Disteche, C. M., Yu, C.-E., Anderson, L., Oshima, J., Nakura, J., Miki, T., Kamino, K., Ogihara, T., Schellenberg, G. D., and Martin, G. M. (1994b). Evidence against DNA polymerase-β as a candidate gene for Werner syndrome. *Hum. Genet.* **93:** 507–512.

Cook, A., Raskind, W., Blanton, S. H., Pauli, R. M., Gregg, R. G., Francomano, C. A., Puffenberg, E., Conrad, E. U., Schmale, G., Schellenberg, G. D., Wijsman, E. J., Hecht, J. T., Wells, D. E., and Wagner, M. J. (1993). Genetic heterogeneity in families with hereditary multiple exocytosis. *Am. J. Hum. Genet.* **53:** 71–79.

Cox, D. R., Burmeister, M., Price, E. R., Kim, S., and Myers, R. M. (1990). Radiation hybrid mapping: A somatic cell genetic method for constructing high-resolution maps of mammalian chromosomes. *Science* **250:** 245–250.

Cox, D. R., Pritchard, C. A., Uglum, E., Casher, D., Kobori, J., and Myers, R. M. (1989). Segregation of the Huntington disease region of human chromosome 4 in a somatic cell hybrid. *Genomics* **4:** 397–407.

Cunningham, C., Dunlop, M. G., Wyllie, A. H., and Bird, C. C. (1993). Deletion mapping in colorectal cancer of a putative tumor suppressor gene in 8p22–p21.3. *Oncogene* **8:** 1391–1396.

Daher, K. A., Lehrer, R. I., Ganz, T., and Kronenberg, M. (1988). Isolation and characterization of human defensin cDNA clones. *Proc. Natl. Acad. Sci. USA* **85:** 7327–7331.

Edelhoff, S., Ayer, D. E., Zervos, A. S., Stingrimsson, E., Jenkins, N. A., Copeland, N. G., Eisenman, R. N., Brent, R., and Disteche, C. M. (1994). Mapping of two genes encoding members of a distinct subfamily of MAX interacting protein: MAD to human chromosome 2 and mouse chromosome 6, and MXI1 to human chromosome 10 and mouse chromosome 19. *Oncogene* **9:** 665–668.

Emi, M., Fujiwara, Y., and Nakamura, Y. (1993). A primary genetic linkage map of 14 polymorphic loci for the short arm of human chromosome 8. *Genomics* **15:** 530–534.

Emi, M., Takahashi, T., Koyama, K., Okui, K., Oshimura, M., and Nakamura, Y. (1992). Isolation and mapping of 88 new RFLP markers on human chromosome 8. *Genomics* **13:** 1261–1266.

Epstein, C. J., Martin, G. M., Schultz, A. L., and Motulsky, A. G. (1966). Werner's syndrome: A review of its symptomatology, natural history, pathologic features, genetics and relationship to the natural aging process. *Medicine* **45:** 177–221.

Fisher, J. H., Emrie, P. A., Drabkin, H. A., Kushnik, T., Gerber, M., Hofmann, T., and Jones, C. (1988). The gene encoding the hydrophobic surfactant protein SP-C is located on 8p and identifies an *Eco*RI RFLP. *Am. J. Hum. Genet.* **43:** 436–441.

Flejter, W. L., Barcroft, C. L., Guo, S.-W., Lynch, E. D., Boehnke, M., Chandrasekharappa, S., Hayes, S., Collins, F. S., Weber, B. L., and Glover, T. W. (1993). Multicolor FISH mapping with *Alu*-PCR-amplified YAC clone DNA determines the order of markers in the *BRCA1* region on chromosome 17q12–q21. *Genomics* **17:** 624–631.

Fong, D., Chan, M. M., Hsieh, W. T., Menninger, J. C., and Ward, D. C. (1992). Confirmation of the human cathepsin B gene (CTSB) assignment to chromosome 8. *Hum. Genet.* **89:** 10–12.

Fukuchi, K., Martin, G. M., and Monnat, R. J., Jr. (1989). Mutator phenotype of Werner syndrome is characterized by extensive deletions. *Proc. Natl. Acad. Sci. USA* **86:** 5893–5897.

Fukuchi, K., Tanaka, K., Kumahara, Y., Marumo, K., Pride, M., Martin, G. M., and Monnat, R. J., Jr. (1990). Increased frequency of 6-thioguanine-resistant peripheral blood lymphocytes in Werner syndrome patients. *Hum. Genet.* **84:** 249–252.

Glasser, S. W., Korfhagen, T. R., Perme, C. M., Pilot-Matias, T. J., Kister, S. E., and Whitsett, J. A. (1988). Two SP-C genes encoding human pulmonary surfactant proteolipid. *J. Biol. Chem.* **263:** 10326–10331.

Gorski, J. L., Boehnke, M., Reyner, E. L., and Burright, E. N. (1992). A radiation hybrid map of the proximal short arm of the human X chromosome spanning incontinentia pigmenti 1 (IP1) translocation breakpoints. *Genomics* **14:** 657–665.

Goto, M., Rubenstein, M., Weber, J., Woods, K., and Drayna, D. (1992). Genetic linkage of Werner's syndrome to five markers on chromosome 8. *Nature* **355:** 735–738.

Guo, S.-W., Boehnke, M., and Flejter, W. L. (1994). Statistical methods for gene map construction by fluorescence *in situ* hybridization (FISH). Manuscript in preparation.

Heinzmann, C., Kirchgessner, T., Kwiterovich, P. O., Ladias, J. A., Derby, C., Antonarakis, S. E., and Lusis, A. J. (1991). DNA polymorphism haplotypes of the human lipoprotein lipase gene: Possible association with high density lipoprotein levels. *Hum. Genet.* **86:** 578–584.

Itoh, N., Terachi, T., Ohta, M., and Seo, M. K. (1990). The complete amino acid sequence of the shorter form of human basic fibroblast growth factor receptor deduced from its cDNA. *Biochem. Biophys. Res. Commun.* **169:** 680–685.

Kaur, G. P., Rinaldy, A., Lloyd, R. S., and Athwal, R. S. (1992). A gene that partially compliments xeroderma pigmentosum group A cells maps to human chromosome 8. *Somatic Cell Mol. Genet.* **18:** 371–379.

Kumar, S., Kimberling, W. J., Kenyon, J. B., Smith, R. J. H., Marres, H. A. M., and Cremers, C. W. R. J. (1992). Autosomal dominant bronchio-oto-renal syndrome-localization of a disease gene to chromosome 8q by linkage in a Dutch family. *Hum. Mol. Genet.* **1:** 491–495.

Lawrence, J. B., Singer, R. H., and McNeil, J. A. (1990). Interphase and metaphase resolution of different distances within the human dystrophin gene. *Science* **249:** 928–932.

Ledbetter, S. A., Nelson, D. L., Warren, S. T., and Ledbetter, D. H. (1990). Rapid isolation of DNA probes within specific chromosome regions by interspersed repetitive sequence polymerase chain reaction. *Genomics* **6:** 475–481.

Lewis, T. B., Leach, R. J., Ward, K., O'Connell, P., and Ryan, S. G. (1993). Genetic heterogeneity in benign familial neonatal convulsions: Identification of a new locus on chromosome 8q. *Am. J. Hum. Genet.* **53:** 670–675.

Lux, S. E., Tse, W. T., Menninger, J. C., John, K. M., Harris, P., Shalev, O., Chilcote, R. R., Marchesi, S. L., Watkins, P. C., Bennett, V., McIntosh, S., Collins, F. S., Francke, U., Ward, D. C., and Forget, B. G. (1990). Hereditary spherocytosis associated with deletion of human erythrocyte ankyrin gene on chromosome 8. *Nature* **345:** 736–739.

Mattei, M. G., Etienne, J., Chuat, J. C., Nguyen, V. C., Brault, D., Bernheim, A., and Galibert, F. (1993). Assignment of the human lipoprotein lipase (LPL) gene to chromosome band 8p22. *Cytogenet. Cell Genet.* **63:** 45–46.

Nakura, J., Miki, T., Nagano, K., Kihara, K., Ye, L., Kamino, K., Fujiwara, Y., Yoshida, S., Murano, S., Fukuchi, K., Wijsman, E. M., Martin, G. M., Schellenberg, G. D., and Ogihara, T. (1993). Close linkage of the gene for Werner's syndrome to ANK1 and D8S87 on the short arm of chromosome 8. *Gerontology* **39**(suppl. 1): 11–15.

Nelson, D. L., Ledbetter, S. A., Corbo, L., Victoria, M. F., Ramirez-Solis, R., Webster, T. D., Ledbetter, D. H., and Caskey, C. T. (1989). *Alu* polymerase chain reaction: A method for rapid isolation of

human-specific sequences from complex DNA sources. *Proc. Natl. Acad. Sci. USA* **86:** 6686–6690.

NIH/CEPH Collaborative Mapping Group (1992). A comprehensive genetic linkage map of the human genome. *Science* **258:** 67–86.

Ohsako, S., and Deguchi, T. (1990). Cloning and expression of cDNAs for polymorphic and monomorphic arylamine *N*-acetyltransferases from human liver. *J. Biol. Chem.* **265:** 4630–4634.

Parrish, J. E., Wagner, M. J., Hecht, J. T., Scott, C. I., Jr., and Wells, D. E. (1991). Molecular analysis of overlapping chromosomal deletions in patients with Langer–Giedion syndrome. *Genomics* **11:** 54–61.

Ruta, M., Burgess, W., Givol, D., Epstein, J., Neiger, N., Kaplow, J., Crumley, G., Dionne, C., Jaye, M., and Schlessinger, J. (1989). Receptor for acidic fibroblast growth factor is related to the tyrosine kinase encoded by the *fms*-like gene (FLG). *Proc. Natl. Acad. Sci. USA* **86:** 8722–8726.

Salk, D., Bryant, E., Hoehn, H., Johnston, P., and Martin, G. M. (1985). Growth characterization of Werner syndrome cells *in vitro*. *Adv. Exp. Med. Biol.* **190:** 305–311.

Schellenberg, G. D., Martin, G. M., Wijsman, E. M., Nakura, J., Miki, T., and Ogihara, T. (1992a). Homozygosity mapping and Werner's syndrome. *Lancet* **339:** 1002.

Schellenberg, G. D., Bird, T. D., Wijsman, E. M., Orr, H. T., Anderson, L., Nemens, E., White, J. A., Bonnycastle, L., Weber, J. L., Alonso, M. E., Potter, H., Heston, L. L., and Martin, G. M. (1992b). Genetic linkage evidence for a familial Alzheimer's disease locus on chromosome 14. *Science* **258:** 668–670.

Siden, T. S., Kumlien, J., Schwartz, C. E., and Rohme, D. (1992). Radiation fusion hybrids for human chromosomes 3 and X generated at various irradiation doses. *Somatic Cell Mol. Genet.* **18:** 33–44.

Smith, R. J. H., Coppage, K. B., Ankerstjerne, J. K. B., Capper, D. T., Kumar, S., Kenyon, J., Tinley, S., Comeau, K., and Kimberling, W. J. (1992). Localization of the gene for branchiootorenal syndrome to chromosome 8q. *Genomics* **14:** 841–844.

Sparkes, R. S., Kronenberg, M., Heinzmann, C., Daher, K. A., Klisak, I., Ganz, T., and Mohandas, T. (1989). Assignment of defensin gene(s) to human chromosome 8p23. *Genomics* **5:** 240–244.

Tamari, M., Hamaguchi, M., Shimizu, M., Oshimura, M., Takayama, H., Kohno, T., Yamaguchi, N., Sugimura, T., Terada, M., and Yokota, J. (1992). Ordering of human chromosome 3p markers by radiation hybrid mapping. *Genomics* **13:** 705–712.

Thomas, W., Rubenstein, M., Goto, M., and Drayna, D. (1993). A genetic analysis of the Werner syndrome region on human chromosome 8p. *Genomics* **16:** 685–690.

Thomas, W., and Drayna, D. (1993). A polymorphic dinucleotide repeat at the D8S339 locus. *Hum. Mol. Genet.* **2:** 828.

Tollefsbol, T. O., and Cohen, H. J. (1984). Werner's syndrome: An underdiagnosed disorder resembling premature aging. *Age* **7:** 75–88.

Tomfohrde, J., Wood, S., Schertzer, M., Wagner, M. J., Wells, D. E., Parrish, J., Sadler, L. A., Blanton, S. H., Daiger, S. P., Wang, Z., Wilkie, P. J., and Weber, J. L. (1992). Human chromosome 8 linkage map based on short tandem repeat polymorphisms: Effect of genotyping errors. *Genomics* **14:** 144–152.

Trask, B. J., Massa, H., Kenwrick, S., and Gitschier, J. (1991). Mapping of human chromosome Xq28 by two-color fluorescence *in situ* hybridization of DNA sequence to interphase cell nuclei. *Am. J. Hum. Genet.* **48:** 1–5.

Trask, B. J., Allen, S., Massa, H., Fertitta, A., Sachs, R., van der Engh, G., and Wu, M. (1994). Studies of metaphase and interphase using fluorescence *in situ* hybridization. 58th CSH Symp. Quant. Biol. Proc., Cold Spring Harbor, NY.

Tutic, M., Lu, X., Schirmer, R. H., and Werner, D. (1990). Cloning and sequencing of mammalian glutathione reductase CDNA. *Eur. J. Biochem.* **188:** 523–528.

Wagner, M. J., Ge, Y., Siciliano, M., and Wells, D. E. (1991). A hybrid cell mapping panel for regional localization of probes to human chromosome 8. *Genomics* **10:** 114–125.

Weber, B., Collins, C., Robbins, C., Magenis, R. E., Delaney, A. D., Gray, J. W., and Hyden, M. R. (1990). Characterization and organization of DNA sequences adjacent to the human telomere associated repeat $(TTAGGG)_n$. *Nucleic Acids Res.* **18:** 3353–3361.

Weissenbach, J., Gyapay, G., Dib, C., Vignal, A., Morissette, J., Millasseau, P., Vaysseix, G., and Lathrop, M. (1992). A second-generation linkage map of the human genome. *Nature* **359:** 794–801.

Westbrook, C. A., Wood, S., and Yaremko, M. L. (1993). Physical localization of STR-positive markers for the short arm of chromosome 8. *Cytogenet. Cell Genet.* **64:** 146.

Williamson, P., Lang, J., and Boyd, Y. (1991). The gonadotropin-releasing hormone (Gnrh) gene maps to mouse chromosome 14 and identifies a homologous region on human chromosome 8. *Somatic Cell Mol. Genet.* **17:** 609–615.

Wood, S., Schertzer, M., Drabkin, H., Patterson, D., Longmire, J. L., and Deaven, L. L. (1992). Characterization of a human chromosome 8 cosmid library constructed from flow sorted chromosomes. *Cytogenet. Cell Genet.* **59:** 243–247.

Yu, C. E., Anderson, L., Oshima, J., and Schellenberg, G. D. (1994a). Dinucleotide repeat polymorphism in a cosmid containing the fibroblast growth factor receptor 1 (FGFR1) gene. *Hum. Mol. Genet.* **3:** 212.

Yu, C. E., Anderson, L., Oshima, J., and Schellenberg, G. D. (1994b). Dinucleotide repeat polymorphism in a cosmid containing the D8S131 locus. *Hum. Mol. Genet.* **3:** 211.